



Cite this: *CrystEngComm*, 2017, 19, 3892

Received 9th May 2017,
Accepted 14th June 2017

DOI: 10.1039/c7ce00881c

rsc.li/crystengcomm

Macrocyclic host cucurbit[6]uril forms supramolecular complexes with dipeptides sequenced as Gly-X (X is either an aromatic amino acid residue Phe, Tyr, and Trp or Gly) in the solid state. Despite exclusion complexation, the interaction between guest dipeptide and host cucurbit[6]uril is multipoint. The ammonium and amide nitrogen atoms of dipeptide participate in hydrogen bonding with a host carbonyl rim and water molecules or chloride anions trapped inside the macrocyclic cavity. The structural study reveals the stabilizing role of the aromatic residues in the supramolecular assembly due to their complementarity with the outer surface of cucurbit[6]uril. In the absence of an aromatic side chain, the calcium ions can stabilize and guide the supramolecular assembly between the macrocycle and Gly-Gly dipeptide.

Cucurbit[n]urils are supramolecular macrocyclic hosts with hydrophobic cavities and two identical carbonyl rimmed portals. Interest in cucurbit[n]urils as containers and supramolecular receptors is increasingly growing due to their excellent recognition and complexation properties in aqueous media.¹ One of the most intriguing aspects of their host-guest chemistry is the recognition of biologically important molecules, such as amino acids, small peptides and even proteins.² Supramolecular approaches that involve cucurbit[n]uril macrocyclic hosts to modify and control protein assembly are particularly attractive and may have important implications in chemical biology.³ Investigation of supramolecular interactions of cucurbit[n]urils with biomolecules is necessary for providing mechanistic insight into their molecular recognition and self-assembly properties and designing new protocols to control and regulate protein activity.⁴ On the other hand, the interaction of these macrocyclic hosts with amino acids and peptides is important in the context of cucurbituril-based drug delivery, as it might affect the stability of cucurbituril-drug complexes, for example ac-

Exploring cucurbit[6]uril-peptide interactions in the solid state: crystal structure of cucurbit[6]uril complexes with glycyl-containing dipeptides†

Oksana Danylyuk

celerating drug release from the host cavity by competitive binding. Moreover, the knowledge about cucurbit[n]uril binding preference towards specific biomolecules (or residues) could be beneficial for drug targeting. Despite remarkable progress in the study of cucurbit[n]uril interactions with amino acids, oligopeptides and even proteins, the X-ray structural investigations of these assemblies are rather scarce,⁵ which may be explained by difficulties in obtaining suitable crystals for X-ray single crystal diffraction, as well as particularly challenging and time-consuming supramolecular crystallography arising from small crystals, poor diffraction, flexibility of the framework manifested in high degrees of structural disorder and often air sensitivity. Despite these difficulties, the structural study of supramolecular systems is worth the effort as the crystal structure provides unequivocal proof for the formation of supramolecular assembly and direct insight into molecular recognition, elucidating interaction mode (geometry, stoichiometry, and non-covalent interactions) between hosts and guests.

In this work, we would like to present our results on the structural study of supramolecular complexes between the macrocyclic host cucurbit[6]uril (CB6) and a series of dipeptides. For our study, we selected glycine and aromatic amino acid containing dipeptides sequenced as Gly-X, where X is either an aromatic amino acid residue (Phe, Tyr, Trp) or Gly. Glycine is the simplest of all twenty amino acids with only hydrogen on its side chain. The lack of a complex side chain allows high flexibility in the proteins and that is why glycine is often found in the loop regions, where the polypeptide chain makes a sharp turn.⁶ Despite its simplicity, glycine is a major building component of many structural proteins, such as collagen,⁷ some spider silks,⁸ silkworm silk⁹ and marine mussel bioadhesives.¹⁰ Aromatic amino acid residues are commonly found at the important binding sites of natural complexes of peptides and proteins.¹¹ The aromatic groups provide a large binding surface/interface and enable several types of intermolecular interactions, such as π -stacking, C-H \cdots π interactions, and hydrophobic binding.

Institute of Physical Chemistry, Polish Academy of Sciences, Kasprzaka 44/52, 01-224 Warsaw, Poland. E-mail: odanylyuk@ichf.edu.pl

† CCDC 1548093–1548096. For crystallographic data in CIF or other electronic format see DOI: 10.1039/c7ce00881c



The first study on the interaction of **CB6** with small peptides in aqueous solution was performed by Buschmann and co-workers in 2005.¹² The dipeptides were found to form exclusion complexes with the N-terminal ammonium groups binding to the **CB6** portal. Early work of Kim and Inoue showed the complexation of dipeptides containing **Phe** by **CB7**.¹³ Later, it was found that **CB7** effectively recognizes peptide sequences **Phe-Gly** over **Gly-Phe** and **Tyr-Gly** over **Gly-Tyr** as well as **Trp-Gly** over **Gly-Trp**.¹⁴ **CB8** has been shown to selectively recognize and bind aromatic tripeptides **Trp-Gly-Gly** and **Phe-Gly-Gly** in aqueous solution.¹⁵ The authors also reported very interesting crystal structures of **CB8** complexes with these tripeptides elucidating the structural basis for selective recognition and unprecedented peptide sequence selectivity. Namely, the crystal structure of a **CB8** complex with **Trp-Gly-Gly** revealed the inclusion of an indole ring into the host macrocyclic cavity and the ion-dipole interactions between the N-terminal nitrogen and carbonyl rim of **CB8**. The crystal structure of a **CB8** complex with **Phe-Gly-Gly** has shown the dimerization of the tripeptide through inclusion of two **Phe** residues interacting *via* π -stacking inside the host cavity. It should be mentioned that these two crystal structures are the first and only structural study on cucurbituril interactions with small peptides. Interestingly, Urbach and co-workers also succeeded in the crystallization of a human insulin complex with **CB7**.¹⁶ The beautiful crystal structure showed that binding occurs at the N-terminal **Phe** residue and that the N-terminus unfolds to enable binding. Kim and co-workers showed that **CB7** prevents the fibrillation of insulin and β -amyloid by capturing **Phe** residues, which are crucial to the hydrophobic interactions formed during amyloid fibrillation.¹⁷

In order to better understand the versatility and capability of cucurbit[n]urils as host molecules towards bioactive guests, particularly amino acids and small peptides, we continue to explore their host-guest supramolecular chemistry in the solid state. Herein, four supramolecular complexes of **CB6** with glycyl-containing dipeptides have been crystallized and their crystal structures have been established *via* single crystal X-ray diffraction. The structural aspects of the host-guest complexation, main non-covalent interactions that guide the assembly, the role of the aromatic residues and the metal ion in the self-assembly and resulting supramolecular architecture in the solid state have been elucidated.

Three complexes **1–3** of **CB6** with aromatic dipeptides **Gly-Phe**, **Gly-Tyr** and **Gly-Trp** crystallized from aqueous solution of **CB6**, the corresponding dipeptide and magnesium chloride used to improve solubility of the macrocycle. Magnesium cations have not been found in the final crystalline assemblies. An attempt to introduce calcium ions into the **CB6**-aromatic dipeptide systems as solubilizing and/or structure-directing agents resulted in the crystallization of the known **CB6** coordination polymer with calcium ions.¹⁸ Crystal structure analysis revealed that all three complexes crystallize in the chiral monoclinic space group *P2*₁ and are isostructural. The dipeptides are in a zwitterionic form and are complexed

exo with respect to the host cavity. An interesting trend found in these three complexes is the slight decrease in the unit cell volume upon enlarging the aromatic residue **Phe** \rightarrow **Tyr** \rightarrow **Trp** (3180, 3159 and 3097 Å³). This trend might suggest more effective packing of **CB6** complexes with larger aromatic systems, thus leading to more efficient interaction between the macrocycle and aromatic Gly-X dipeptide in the solid state. The careful crystal structure analysis revealed that the main host-guest binding motif in all three complexes involves a highly polar **CB6** rim and two nitrogen atoms of dipeptide – terminal ammonium and amido nitrogen of the peptide bond, Fig. 1. The main structural features, non-covalent interactions and supramolecular organization in the resulting assemblies will be discussed on the example of **CB6** complex **1** with **Gly-Phe**.

The asymmetric unit of complex **1** comprises one **CB6** molecule, one dipeptide **Gly-Phe** as a zwitterion and fourteen water molecules. The dipeptide is complexed at one of the **CB6** rims leaving the second identical rim not involved in the host-guest interaction. The **CB6** macrocyclic cavity is occupied with two water molecules. The dipeptide adopts conformation suitable for the interaction with the **CB6** carbonyl rim *via* both ammonium and amido nitrogen atoms. The terminal ammonium of **Gly-Phe** lies in the plane of six carbonyl oxygen atoms of the host and donates hydrogen bonds to three oxygen atoms (one of the H-bonds is bifurcated, N-HO distances are 2.76, 2.88 and 3.03 Å). The fourth hydrogen bond is realized towards water molecules included deeply in the macrocyclic cavity (2.79 Å). The amido nitrogen of the

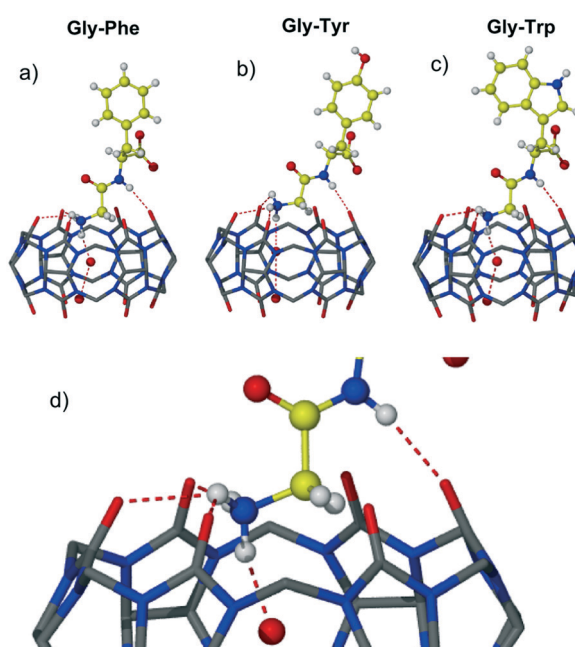


Fig. 1 The host-guest complexes **1–3** of **CB6** with dipeptides a) **Gly-Phe**; b) **Gly-Tyr**; c) **Gly-Trp**; d) zoom on the main host-guest binding motif; hydrogen bonds between ammonium and amide nitrogen atoms of dipeptide and carbonyl oxygen atoms of **CB6** as red dashed lines, note the additional hydrogen bonding of dipeptide ammonium with a water molecule included in the macrocyclic cavity.



dipeptide also forms hydrogen bond with carbonyl oxygen of the host ($\text{N}-\text{H}\cdots\text{O}$ distance 2.88 Å). The aromatic group of the **Phe** residue is directed away from the host portal and is positioned almost perpendicular to the CB6 rim; the dihedral angle between the guest phenyl group and plane defined by six carbonyl oxygen atoms of CB6 is 86°. The carboxylate and carbonyl groups of **Gly-Phe** are involved in rich hydrogen bonding with water molecules.

Further symmetry expansion shows that the aromatic group of the **Phe** residue is in close contact with the outer surface of two CB6 macrocycles in the crystal lattice. The aromatic moiety of the dipeptide contributes to the overall assembly through $\text{C}-\text{H}\cdots\pi$ interactions between backbones of adjacent CB6 and the aromatic system of **Gly-Phe**, Fig. 2a. There are one methine and one methylene carbon atoms from one CB6 and one methine carbon atom from another CB6 in close contact with the **Phe** aromatic residue enabling $\text{C}-\text{H}\cdots\pi$ interactions. Additionally, there are two $\text{C}-\text{H}\cdots\text{O}$ weak hydrogen bonds between methine carbon atoms of CB6 and a carboxyl oxygen atom of the dipeptide ($\text{C}-\text{H}\cdots\text{O}$ distance is 3.22 and 3.23 Å). When comparing similar host-guest organization in CB6 complex 3 with **Gly-Trp**, it is evident that there are more contact points between the CB6

outer surfaces and large indole system of **Trp**, Fig. 2b. Moreover, the third CB6 takes part in the interaction with an enlarged aromatic moiety, in this way, making overall supramolecular packing more efficient.

The second portal of CB6 is not engaged in the interaction with dipeptide and is closed with the backbone of the adjacent macrocycle in the T-shaped geometry. Such a 'side to portal' arrangement of cucurbiturils is quite favorable because of the multiple CH_2 (methylene) and CH (methine) weak hydrogen bonds with carbonyl oxygen atoms of the adjacent macrocycle. The T-shaped arrangement is realized in many cucurbituril crystalline hydrates as well as in some of their host-guest and even coordination complexes.¹⁹ These multipoint interactions are believed to be responsible for the solid-state assembly of CBs, their excellent thermal and chemical stability, and low water solubility. The supramolecular organization of adjacent CB6 molecules in complex 1 is depicted in Fig. 3a which represents zigzag strands of CB6-dipeptide units running along the *b* direction. The host molecules are arranged in a 'side to portal' manner and guest dipeptides protrude from other portals of CB6s. The adjacent zigzag strands are arranged in a parallel way and stitched together by $\text{C}-\text{H}\cdots\pi$ interactions between CB6 and aromatic groups of dipeptide, Fig. 3b.

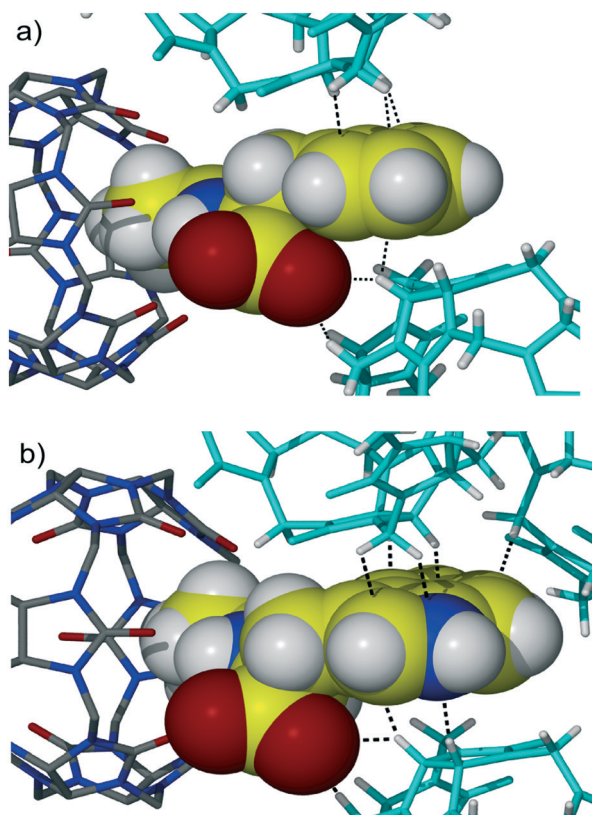


Fig. 2 The interaction of the aromatic group of dipeptide (a) **Gly-Phe** and (b) **Gly-Trp** with the outer surfaces of CB6 (macrocycles coloured in blue) in the crystal lattice. $\text{C}-\text{H}\cdots\pi$ and $\text{C}-\text{H}\cdots\text{O}$ weak hydrogen bonds between methine and methylene carbon atoms of CB6 and the aromatic system of dipeptide depicted as dashed black lines. Note the increase in the number of these contacts in the case of **Gly-Trp** (b).

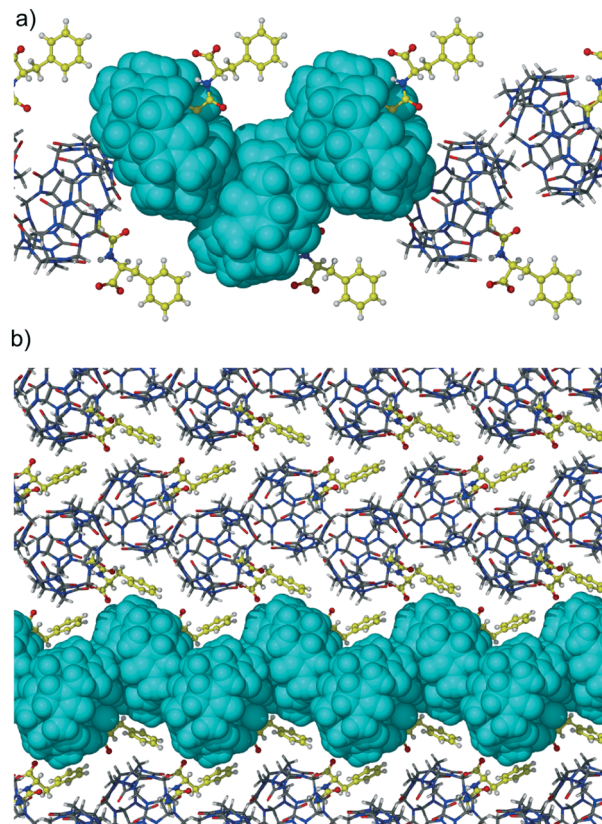


Fig. 3 (a) The supramolecular organization of CB6 complex 1 with **Gly-Phe** in zigzag strands running along the *b* direction. The adjacent CB6 molecules are in T-shaped geometry arising from 'side to portal' self-association of the macrocycles; (b) the packing of the CB6 complex with **Gly-Phe** viewed along the *a* direction.



The crystallization protocol used for obtaining CB6 complexes **1–3** with aromatic dipeptides was not successful in the case of the Gly-Gly guest. It is not surprising as this simple dipeptide differs significantly from the previously employed Gly-X aromatic dipeptides – it is achiral and lacks an aromatic side chain that obviously contributes significantly to the stabilization of the CB6-dipeptide assembly. The change of the salt used for enhancing CB6 aqueous solubility from magnesium chloride to calcium chloride resulted in the crystallization of the desired compound **4**. The CB6 complex with Gly-Gly crystallized in the tetragonal space group $I4_1/a$. X-ray analysis revealed that calcium ions are embedded in the crystal lattice of the complex and are active participants in the overall supramolecular assembly. It should be mentioned that metal ions are frequently found in the protein structures and are often necessary for protein stability, structure and function.²⁰ Moreover, the presence of metal ions is often necessary for protein crystallization.

The asymmetric unit of multi-component complex **4** comprises half of the CB6 molecule lying over an inversion centre, one Gly-Gly dipeptide in the zwitterionic form, one quarter of a calcium cation positioned on the 4-fold rotoinversion axis, half of a chloride anion and water molecules. The crystal structure is characterized by substantial disorder of several components: the Gly-Gly dipeptide was modeled as disordered over two positions, water molecules constituting the coordination sphere of the calcium ion are disordered because of their position close to the rotoinversion axis, chloride anions occupying the macrocyclic cavity are also disordered, and additionally, disordered lattice water molecules are present. The calcium cation is coordinated by disordered aqua ligands, the coordination number of the metal ion is six, and the coordination polyhedron of calcium is the distorted tetragonal bipyramidal. The metal–oxygen distances are in the range of 2.26–2.49 Å and typical to those found in the literature.²¹

Different from 1:1 CB6 complexes with aromatic Gly-X dipeptides, here, Gly-Gly is complexed at each portal of the macrocycle giving 1:2 host–guest assembly, Fig. 4. The host–guest main binding motif is again the interaction of terminal

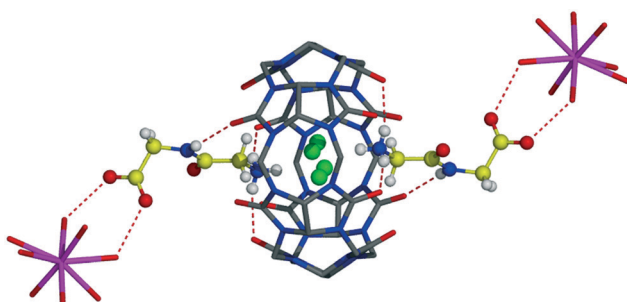


Fig. 4 Host–guest complex **4** of CB6 with Gly-Gly dipeptide. The CB6 cavity is occupied with disordered chloride anions (coloured in green); calcium aqua complexes (calcium ion in violet) take part in the stabilization of the assembly by hydrogen bonding with carboxylate groups of dipeptide.

ammonium and amide nitrogen atoms of dipeptide with carbonyl oxygen atoms of CB6 *via* ion–dipole and hydrogen bonding. Surprisingly, the CB6 cavity is taken by chloride anions. We have already observed similar trapping of chloride anions by a CB6 cavity in a solid-state complex with tryptophan.^{5c} The inclusion of chloride anions is stabilized by charge-assisted N–H···Cl hydrogen bonding with ammonium functions of two Gly-Gly dipeptides closing each portal of CB6 (N–H···Cl distances are in the range of 2.94–3.12 Å). The carboxylate group of dipeptide is involved in hydrogen bonding with aqua ligands of a calcium cation thus providing stabilization to the overall supramolecular assembly, Fig. 5a.

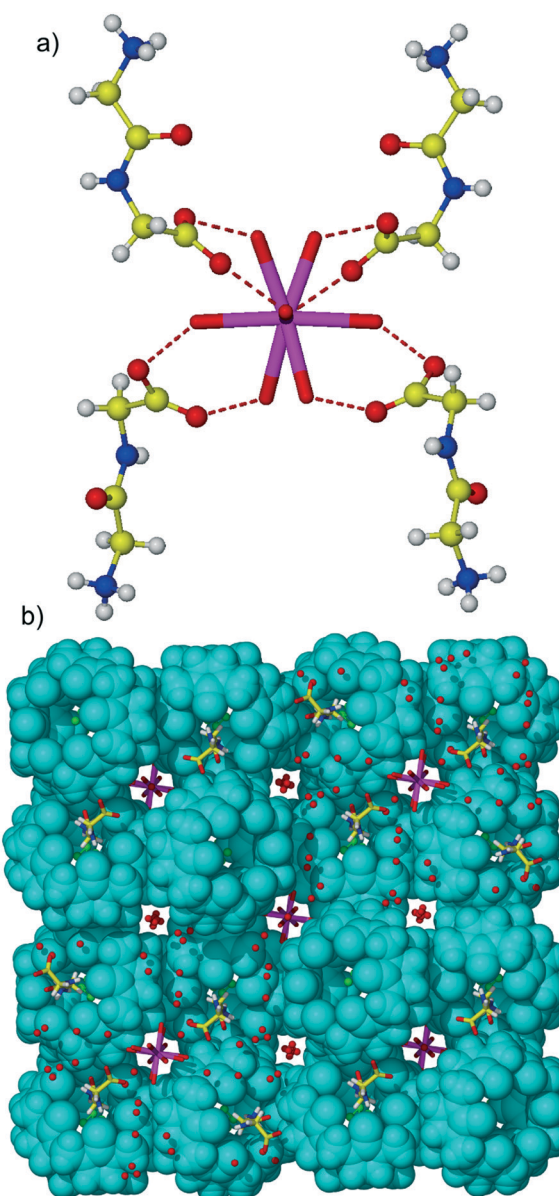


Fig. 5 (a) The hydrogen bonding between aqua ligands of a calcium ion and carboxylate functions of Gly-Gly dipeptide in complex **4**; each aqua complex interacts with four dipeptides. Only one of the disordered positions of aqua ligands and dipeptide has been shown; (b) packing of complex **4** along the *c* direction.



Each aqua-coordinated calcium interacts with four Gly-Gly dipeptides, donating two hydrogen bonds to each carboxylate group. Such interaction mode generates tubular organization of the multi-component assembly in the solid state, Fig. 5b. The tube formed of CB6 and Gly-Gly molecules assembles around aqua-coordinated calcium cations.

To conclude, the solid-state complexes of CB6 with dipeptides sequenced as Gly-X (X is Phe, Tyr, Trp or Gly) show a number of interesting structural features. Despite exclusion complexation, the interaction of the CB6 macrocycle with dipeptides is multipoint. It involves ion-dipole interaction, hydrogen bonding between ammonium and amido nitrogen atoms of the dipeptide with the polar carbonyl rim of CB6, hydrogen bonding of the ammonium nitrogen of the dipeptide with water molecules or chloride anions trapped inside the macrocyclic cavity. The crystal structure analysis revealed the stabilizing role of aromatic residues in the supramolecular assembly due to their complementarity with the outer surface of the CB6 skeleton. In the absence of an aromatic side chain, the metal ion can stabilize and guide the supramolecular assembly between CB6 and Gly-Gly dipeptide. The role of calcium ions is mainly in engaging the carboxylate group of dipeptide *via* hydrogen bonding with aqua ligands. Although much work remains to be done to explore the structural supramolecular chemistry of cucurbituril macrocycles with different peptides, the present work suggests potential design strategies for CB6 assemblies with peptide chains – the preference of aromatic residues to be surrounded with outer skeletons of CB6 when the size of the macrocycle does not enable the formation of the inclusion complex and the use of the metal ion as a structure-directing agent in the absence of other structure stabilizing elements.

Experimental

Crystallization

The dipeptides Gly-Gly, Gly-Phe, Gly-Tyr and Gly-Trp were purchased from Sigma Aldrich. CB6 was synthesized according to a literature procedure [A. Day *et al.*, *J. Org. Chem.*, 2001, **66**, 8094].

Complexes 1–3

CB6·10H₂O (10 mg, 8.5 µmol) and MgCl₂·6H₂O (173 mg, 0.85 mmol) were dissolved in distilled water (1 ml) upon gentle heating. The solution of dipeptide Gly-Phe, Gly-Tyr or Gly-Trp (2 equivalents) in 1 ml of water was added to the solution of the macrocycle. The diffraction quality crystals were formed after several days.

Complex 4

CB6·10H₂O (10 mg, 8.5 µmol) and CaCl₂·2H₂O (12.5 mg, 0.085 mmol) were dissolved in distilled water (1 ml) upon gentle heating. The solution of dipeptide Gly-Gly (2 equivalents) in 1 ml of water was added to the solution of the

macrocycle. The diffraction quality crystals were formed after several days.

Single crystal X-ray diffraction

The crystals were selected under Paratone-N oil, mounted on the nylon loops and positioned in the cold stream on the diffractometer. Uniformity of the samples was checked by unit cell determination of several crystals for each sample. The X-ray data for complexes 1, 2 and 4 were collected on a Nonius KappaCCD diffractometer using MoKα radiation ($\lambda = 0.71073$ Å). The data were processed with HKL2000.²² The X-ray data for complex 3 were collected on a SuperNova Agilent diffractometer using CuKα radiation ($\lambda = 1.54184$ Å). The data were processed with CrysAlisPro.²³ Structures were solved by direct methods and refined using SHELXL.²⁴ The figures were prepared using X-Seed²⁵/POV-Ray.

Crystal data for 1. C₄₇H₅₀N₂₆O₃₀, $M_r = 1459.1$, colourless, monoclinic, space group P2₁, $a = 12.8276(3)$, $b = 15.6361(4)$, $c = 16.4483(4)$ Å, $\beta = 105.384(1)$ °, $V = 3180.9(1)$ Å³, $Z = 2$, $\rho_{\text{calc}} = 1.52$ g cm⁻³, $\mu(\text{MoK}\alpha) = 0.13$ mm⁻¹, $\theta_{\text{max}} = 28.2$ °, 47 337 reflections measured, 15 276 unique, 929 parameters, $R = 0.083$, $wR = 0.205$ ($R = 0.094$, $wR = 0.213$ for all data), GooF = 1.09. CCDC 1548093.

Crystal data for 2. C₄₇H₅₀N₂₆O_{29.5}, $M_r = 1451.1$, colourless, monoclinic, space group P2₁, $a = 12.8204(14)$, $b = 15.4423(9)$, $c = 16.4045(11)$ Å, $\beta = 103.346(4)$ °, $V = 3159.7(4)$ Å³, $Z = 2$, $\rho_{\text{calc}} = 1.52$ g cm⁻³, $\mu(\text{MoK}\alpha) = 0.13$ mm⁻¹, $\theta_{\text{max}} = 29.0$ °, 49 148 reflections measured, 16 170 unique, 1151 parameters, $R = 0.081$, $wR = 0.181$ ($R = 0.122$, $wR = 0.210$ for all data), GooF = 1.11. CCDC 1548094.

Crystal data for 3. C₄₉H₅₁N₂₇O_{27.5}, $M_r = 1458.2$, colourless, monoclinic, space group P2₁, $a = 12.6736(2)$, $b = 15.6598(2)$, $c = 16.4846(3)$ Å, $\beta = 108.761(2)$ °, $V = 3097.81(9)$ Å³, $Z = 2$, $\rho_{\text{calc}} = 1.56$ g cm⁻³, $\mu(\text{CuK}\alpha) = 1.13$ mm⁻¹, $\theta_{\text{max}} = 71.9$ °, 21 272 reflections measured, 11 900 unique, 1182 parameters, $R = 0.065$, $wR = 0.179$ ($R = 0.067$, $wR = 0.182$ for all data), GooF = 1.03. CCDC 1548096.

Crystal data for 4. C₂₂H₂₆Ca_{0.25}Cl_{0.5}N₁₄O_{18.4}, $M_r = 808.3$, colourless, tetragonal, space group I4₁/a, $a = 31.3154(5)$, $c = 14.3835(2)$ Å, $V = 14105.4(5)$ Å³, $Z = 16$, $\rho_{\text{calc}} = 1.52$ g cm⁻³, $\mu(\text{MoK}\alpha) = 0.20$ mm⁻¹, $\theta_{\text{max}} = 26.4$ °, 13 959 reflections measured, 7167 unique, 673 parameters, $R = 0.077$, $wR = 0.208$ ($R = 0.091$, $wR = 0.223$ for all data), GooF = 1.03. CCDC 1548095.

References

1. J. W. Lee, S. Samal, N. Selvapalam, H.-J. Kim and K. Kim, *Acc. Chem. Res.*, 2003, **36**, 621; E. Masson, X. Ling, R. Joseph, L. Kyeremeh-Mensah and X. Lu, *RSC Adv.*, 2012, **2**, 1213; X.-L. Ni, X. Xiao, H. Cong, L.-L. Liang, K. Cheng, X.-J. Cheng, N.-N. Ji, Q.-J. Zhu, S.-F. Xue and Z. Tao, *Chem. Soc. Rev.*, 2013, **42**, 9480; X.-L. Ni, X. Xiao, H. Cong, Q.-J. Zhu, S.-F. Xue and Z. Tao, *Acc. Chem. Res.*, 2014, **47**, 1386; K. I. Assaf and W. M. Nau, *Chem. Soc. Rev.*, 2015, **44**, 394.

2 S. J. Barrow, S. Kasera, M. J. Rowland, J. del Barrio and O. A. Scherman, *Chem. Rev.*, 2015, **115**, 12320.

3 F. de Greef, M. Merkx and L. Brunsved, *Angew. Chem., Int. Ed.*, 2016, **55**, 8899; S. Sankaran, M. C. Kiren and P. Jonkheijm, *ACS Nano*, 2015, **9**(4), 3579.

4 C. Hou, Z. Huang, Y. Fang and J. Liu, *Org. Biomol. Chem.*, 2017, **15**, 4272.

5 J.-M. Yi, Y.-Q. Zhang, H. Cong, S.-F. Xue and Z. Tao, *J. Mol. Struct.*, 2009, **933**, 112; P. Thuery, *Inorg. Chem.*, 2011, **50**(21), 10558; O. Danylyuk and V. P. Fedin, *Cryst. Growth Des.*, 2012, **12**(2), 550; Z.-Z. Gao, R.-L. Lin, D. Bai, Z. Tao, J.-X. Liu and X. Xiao, *Sci. Rep.*, 2017, **7**, 44717; P.-H. Shan, S.-C. Tu, R.-L. Lin, Z. Tao, J.-X. Liu and X. Xiao, *CrystEngComm*, 2017, **19**, 2168.

6 F. Krieger, A. Möglich and T. Kieffhaber, *J. Am. Chem. Soc.*, 2005, **127**(10), 3347.

7 M. D. Shoulders and R. T. Raines, *Annu. Rev. Biochem.*, 2009, **78**, 929.

8 J. D. van Beek, S. Hess, F. Vollrath and B. H. Meier, *Proc. Natl. Acad. Sci. U. S. A.*, 2002, **99**(16), 10266.

9 T. Asakura, T. Ito, M. Okudaira and T. Kameda, *Macromolecules*, 1999, **32**(15), 4940.

10 K. J. Coyne, X.-X. Qin and J. H. Waite, *Science*, 1997, **277**(5333), 1830.

11 B. Ma, T. Elkayam, H. Wolfson and R. Nussinov, *Proc. Natl. Acad. Sci. U. S. A.*, 2003, **100**(10), 5772.

12 H.-J. Buschmann, L. Mutihac, R.-C. Mutihac and E. Schollmeyer, *Thermochim. Acta*, 2005, **430**(1-2), 79.

13 M. V. Rekharsky, H. Yamamura, C. Inoue, M. Kawai, I. Osaka, R. Arakawa, K. Shiba, A. Sato, Y. Ho Ko, N. Selvapalam, K. Kim and Y. Inoue, *J. Am. Chem. Soc.*, 2006, **128**, 14871.

14 M. V. Rekharsky, H. Yamamura, Y. H. Ko, N. Selvapalam, K. Kim and Y. Inoue, *Chem. Commun.*, 2008, 2236.

15 L. M. Heitmann, A. B. Taylor, P. J. Hart and A. R. Urbach, *J. Am. Chem. Soc.*, 2006, **128**(38), 12574.

16 J. M. Chinai, A. B. Taylor, L. M. Ryno, N. D. Hargreaves, C. A. Morris, P. J. Hart and A. R. Urbach, *J. Am. Chem. Soc.*, 2011, **133**(23), 8810.

17 H. H. Lee, T. S. Choi, S. J. C. Lee, J. W. Lee, J. Park, Y. H. Ko, W. J. Kim, K. Kim and H. I. Kim, *Angew. Chem., Int. Ed.*, 2014, **53**, 7461.

18 W. A. Freeman, W. L. Mock and N.-Y. Shih, *J. Am. Chem. Soc.*, 1981, **103**, 7367.

19 D. Bardelang, K. A. Udachin, D. M. Leek, J. C. Margeson, G. Chan, C. I. Ratcliffe and J. A. Ripmeester, *Cryst. Growth Des.*, 2011, **11**, 5598; O. Danylyuk, V. P. Fedin and V. Sashuk, *CrystEngComm*, 2013, **15**, 7414; O. Danylyuk, V. P. Fedin and V. Sashuk, *Chem. Commun.*, 2013, **49**, 1859.

20 T. Dudev and C. Lim, *Chem. Rev.*, 2014, **114**, 538.

21 H. Zheng, M. Chruszcz, P. Lasota, L. Lebioda and W. Minor, *J. Inorg. Biochem.*, 2008, **102**, 1765.

22 Z. Otwinowski and W. Minor, *Methods Enzymol.*, 1997, **276**, 307.

23 Agilent Technologies, *CrysAlisPro*, Version 1.171.36.32.

24 G. M. Sheldrick, *Acta Crystallogr., Sect. A: Found. Crystallogr.*, 2008, **64**, 112.

25 L. J. Barbour, *J. Supramol. Chem.*, 2001, **1**, 189–191.

